## Supplemental materials

# Endoplasmic reticulum-associated degradation is required for nephrin maturation and kidney glomerular filtration function

Sei Yoshida[1,2,10] *, Xiaoqiong Wei[1,10], Gensheng Zhang[1,10], Christopher L. O'Connor[3], Mauricio Torres[1], Zhangsen Zhou[1], Liangguang Lin[1], Rajasree Menon[3], Xiaoxi Xu[4], Wenyue Zheng[2], Yi Xiong[5], Edgar Otto[3], Chih-Hang Anthony Tang[6], Rui Hua[2], Rakesh Verma[3], Hiroyuki Mori[1], Yang Zhang[7], Chih-Chi Andrew Hu[6], Ming Liu[4], Puneet Garg[3], Jeffrey B. Hodgin[8], Shengyi Sun[5], Markus Bitzer[3], Ling Qi[1,9] *

## SUPPLEMENTAL METHODS

### A. Human studies

**Single cell RNA-sequencing (scRNA-Seq) analysis of human kidneys**

Human kidney tissue obtained from the unaffected, tumor distant site of a 43 year-old male patient undergoing nephrectomy (warm and cold ischemic time < 5 minutes). Tissue was enzymatically (Liberase TL) and mechanically dissociated as previously described for human developing kidney tissue (1) to generate single cell suspensions. Single cell data was generated using droplet based high-throughput 10XGenomics™ Chromium™ technology. cDNA Libraries were prepared according to manufacturer's protocol and sequenced by the University of Michigan Advanced Genomics Core facility as asymmetric paired end runs (26x115 bases) with a median of 100 million raw sequencing reads per sample. The output from the sequencer was first processed by CellRanger, the proprietary 10X Chromium single cell gene expression analysis software (https://support.10xgenomics.com/single-cell-gene-expression/software/pipelines/latest/what-is-cell-ranger). Data analyses were performed on the CellRanger output data files using Seurat (version 3) R package (https://cran.r-project.org/web/packages/Seurat/index.html). As a quality control step, cells with less than 500 genes and more than 5000 genes were filtered out. The downstream analysis steps include normalization, identification of highly variable genes across the single cells, scaling based on number of UMI and batch effect, principal component analysis, dimensionality reduction (Uniform Manifold Approximation and Projection), batch integration, standard unsupervised clustering, and the discovery of differentially expressed cell-type specific markers. Differential gene expression was used to identify cell-type specific genes using the non-parametric Wilcoxon rank sum test. Raw scRNA-seq data have been deposited in the NCBI with the accession number PRJNA700694 (https://www.ncbi.nlm.nih.gov/bioproject/700694).

**Imaging data analysis**

Five samples (2 healthy donors and 3 FSGS patients) were prepared and imaged in the same way. Five glomerulus images were randomly selected from each sample for quantitation. Podocytes were identified based on the WT1-positive staining as well as their location in glomerulus. Signal intensity of SEL1L/HRD1 per podocyte was measured using ImageJ, which was further analyzed using ggplot2 (ggplort.tidyverse.org). Graphs were plotted with ggplot2. Kruskal-Wallis H test was used for statistical analysis.

## B. Mouse studies

### Quantitation of urine albumin and creatinine

Urine samples were collected from mice at different ages. Urine creatinine was quantitated using mouse Creatinine Colorimetric Assay kit (Cayman Chemical, 500701). Urine albumin was measured using mouse Albumin ELISA kit (Bethyl Laboratories Inc., E99-134). Urine albumin excretion was expressed as the ratio of urine albumin to creatinine. For the Coomassie Blue staining of urinary proteins, 0.5 µl of urine was denatured with 2x sample buffer and then resolved on SDS-PAGE, followed by Coomassie blue staining and quantitation using ImageJ bundled with Java 1.8.0_172 (NIH, USA).

### Blood sample analysis

Mice were anesthetized with isoflurane and blood samples were collected through inferior vena cava and centrifuged at 3000 rpm for 10 min at 4 °C. The supernatants (serum) were transferred to new tubes and sent to the University of Michigan In-Vivo Animal Core for the blood analysis – which included the measurements of creatinine, blood urea nitrogen (BUN), cholesterol, and alanine aminotransferase (ALT).

### Protein lysate preparation

Kidneys or cells were collected, immediately frozen in liquid nitrogen and kept at -80 °C. Frozen kidney tissues or cells were lysed in a buffer containing 50 mM Tris- HCl (pH 7.5), 1% Triton X-100, 1 mM EDTA, 150 mM NaCl and protease inhibitor cocktail, incubated on ice for 30 min, and centrifuged at 13,000 rpm for 10 min at 4 °C. Protein concentrations were measured by using the Bio-Rad BCA assay. For reducing SDS-PAGE, lysates were mixed with 5X denaturing sample buffer (250 mM Tris HCl pH 6.8, 1% SDS, 50% glycerol, 1.44 M β-mercaptoethanol and 0.05% bromophenyl blue). For non-reducing SDS-PAGE, lysates were prepared in 5X non-denaturing sample buffer (250 mM Tris HCl pH 6.8, 1% SDS, 50% glycerol and 0.05% bromophenyl blue). Samples were then heated at 95 °C for 5 min prior to be loaded onto SDS-PAGE.

### Endoglycosidase H (EndoH) and PNGase F treatment

EndoH and PNGase F (New England BioLabs, P0702L and P0704L) treatment were performed according to manufacture's protocols as previously described (2). Briefly, kidney or cell lysates were prepared as described in the lysate section. Following the addition of glycoprotein denaturing buffer (New England BioLabs), lysates were incubated at 100 °C for 10 min, and

then digested with EndoH or PNGase F at 37 °C for 1 hr. The reaction was stopped by the addition of 5X denaturing sample buffer and boiled at 95 °C for 5 min prior to be loaded onto SDS-PAGE.

**Immunoprecipitation (IP)**

Kidneys or cells were homogenized in the NP-40 lysis buffer containing 25 mM Tris-HCl (pH 7.5), 1% NP40, 150 mM NaCl and protease and phosphatase inhibitors, incubated on ice for 1-2 hr and centrifuged at 13,000 rpm for 10 min at 4 °C. Equal amount of protein lysates were incubated with nephrin antibody (ABclonal, A3048), GFP antibody (Santa Cruz, sc-8334) or IgG (Cell Signaling Technology, 2729S) at 4 °C overnight and then followed by protein A agarose beads (Invitrogen 15918-014) for 2 hr at 4 °C. Beads were washed three times with lysis buffer, boiled for 5 min in 2X SDS sample buffer and loaded onto SDS-PAGE gels for western blot analysis.

**Microsomal fractionation**

Half of a frozen kidney was homogenized 15-20 times in a dounce grinder with 1 ml buffer A (50 mM Tris-HCl pH 8.0, 1 mM $\beta$-mercaptoethanol, 1 mM EDTA, 0.32 M sucrose, protease inhibitor and protein phosphatase inhibitor), and centrifuged at 800 g for 10 min. The supernatant (as "Total lysates") was then centrifuged at 4,500 g for 10 min followed by two spins at 16,000 g for 10 min. To collect microsomes (e.g. the ER, Golgi and plasma membranes), the supernatant was diluted to 3 ml in buffer A and centrifuged at 105,000 g for 1 h (Optima MAX-XP, Beckman). The pellet, the microsomal fraction, was dissolved in 80 µl lysis buffer (50 mM Tris-HCl pH 7.5, 150 mM NaCl, 1% NP-40, 1 mM dithiothreitol, protease and protein phosphatase inhibitors), and, together with the supernatant (the cytosol fraction), were quantified using the BCA protein assay and adjusted to the same protein concentration.

## C. In vitro studies

**Immunofluorescence staining in cells**

IF staining of nephrin/KDEL in cells was performed as previously described (3, 4). Briefly, cells, either human podocytes or HEK293T cells transfected with nephrin G270C, were washed with PBS and fixed for 30 min at room temperature with fixation buffer (20 mM HEPES, pH 7.4, 2% PFA, 4.5% sucrose, 70 mM NaCl, 10 mM KCL, 10 mM $MgCl_2$, and 10 mM Sodium Periodate). The fixed cells were then rinsed with TBST, permeabilized with ice-cold methanol for 20 sec and blocked with the blocking buffer (TBST with 5 % BSA) for 30 min at room temperature. Samples

were incubated with primary nephrin antibody diluted in the blocking buffer at 4 °C overnight. After washing three times with TBST for 10 min each, samples were incubated with secondary antibody diluted in blocking buffer for 2 hr at room temperature. Samples were mounted on a slide and examined under a confocal microscope.

**Substrate ubiquitination experiment**

Substrate ubiquitination assay was performed previously described (5). Briefly, HEK293T cells were lysed in NP-40 lysis buffer (50 mM Tris-HCl pH7.5, 1% NP-40, 150 mM NaCl, 1 mM EDTA, protease and protein phosphatase inhibitor cocktails, and 10mM N-ethymaleimide). Equal amount of protein lysates was incubated with antibody-conjugated agarose beads overnight at 4 ℃ with gentle rocking (anti-HA agarose beads, Sigma A2095; anti-Myc agarose beads, Thermo Scientific 20168). Immunocomplexes were washed (137 mM NaCl, 2 mM EDTA, 20 mM Tris- HCl pH 7.5, 10% glycerol) and eluted under denaturing or non-denaturing sample buffer prior to be loaded onto SDS-PAGE for western blot.

**Quantitation of western blot and pulse-chase data**

ImageJ bundled with Java 1.8.0_172 (NIH, USA) was used to substrate background with the default settings (rolling ball radius=50) and then measure the density value of each band.

## D. Studies of disease mutants

**Structure analysis**

C-I-TASSER (6) was used to predict the structures of wildtype and mutant nephrin. Based on these predicted structure models, EvoEF2 (7) was applied to analyze the impact of mutations on the protein folding in terms of $\Delta\Delta G$, i.e. the free energy change caused by single mutation. All the structure images were rendered by PyMOL (version 2.3.2).

**Detergent NP-40 solubility assay**

This assay was performed as previously described (5) to fractionate detergent soluble and insoluble fractions. Briefly, kidneys or cells were lysed on the ice with NP-40 lysis buffer (50 mM Tris-HCl pH 8.0, 0.5% NP-40, 150mM NaCl, 5 mM $MgCl_2$, 10mM N-ethylmaleimide) supplemented with protease inhibitor cocktail. Then the lysate was centrifuged at 12,000× *g* for 10min at 4 °C and the supernatant was collected as NP-40S fraction. The pellet was washed with lysis buffer and then resuspended in 1× SDS sample buffer (50 mM Tris-Cl, 2% SDS, 0.29

M 2-mecaptoethanol, 10% glycerol, 0.01% bromophenyl blue), heated at 95 °C for 30 min and collected as the NP-40P fraction. The NP-40S and NP-40P fractions were subsequently loaded onto SDS-PAGE.

**References:**


1. Menon R, Otto EA, Kokoruda A, Zhou J, Zhang Z, Yoon E, Chen YC, Troyanskaya O, Spence JR, Kretzler M, and Cebrian C. Single-cell analysis of progenitor cell dynamics and lineage specification in the human fetal kidney. *Development.* 2018;145(16).
2. Sha H, Sun S, Francisco AB, Ehrhardt N, Xue Z, Liu L, Lawrence P, Mattijssen F, Guber RD, Panhwar MS, Brenna JT, Shi H, Xue B, Kersten S, Bensadoun A, Peterfy M, Long Q, and Qi L. The ER-associated degradation adaptor protein Sel1L regulates LPL secretion and lipid metabolism. *Cell Metab.* 2014;20(3):458-70.
3. Yoshida S, Pacitto R, Yao Y, Inoki K, and Swanson JA. Growth factor signaling to mTORC1 by amino acid-laden macropinosomes. *J Cell Biol.* 2015;211(1):159-72.
4. Kim GH, Shi G, Somlo DRM, Haataja L, Soon S, Long Q, Nillni EA, Low MJ, Arvan P, Myers MG, and Qi L. Hypothalamic ER-associated degradation regulates POMC maturation, feeding and age-associated obesity. *J Clin Invest.* 2018;128(3):1125-40.
5. Sun S, Shi G, Sha H, Ji Y, Han X, Shu X, Ma H, Inoue T, Gao B, Kim H, Bu P, Guber RD, Shen X, Lee AH, Iwawaki T, Paton AW, Paton JC, Fang D, Tsai B, Yates Iii JR, Wu H, Kersten S, Long Q, Duhamel GE, Simpson KW, and Qi L. IRE1a is an endogenous substrate of endoplasmic-reticulum-associated degradation. *Nat Cell Biol.* 2015;17(12):1546-55.
6. Zheng W, Li Y, Zhang C, Pearce R, Mortuza SM, and Zhang Y. Deep-learning contact-map guided protein structure prediction in CASP13. *Proteins.* 2019;87(12):1149-64.
7. Huang X, Pearce R, and Zhang Y. EvoEF2: Accurate and fast energy function for computational protein design. *Bioinformatics.* 2019;36(4):1135-42.

## SUPPLEMENTAL FIGURES AND LEGENDS

**Figure S1. ScRNA-seq analysis of ERAD and other related ER genes in human kidneys.** **(A)** Visualization of t-distributed stochastic neighbor embedding (tSNE) plot of human renal cells (total 2,545 cells from one normal kidney). **(B-E)** Violin plots for *SEL1L* (B) and *HRD1* (*SYVN1*) (C), IRE1a (ERN1, D) and BiP (HSPA5, E) gene expression in scRNA-seq analysis.

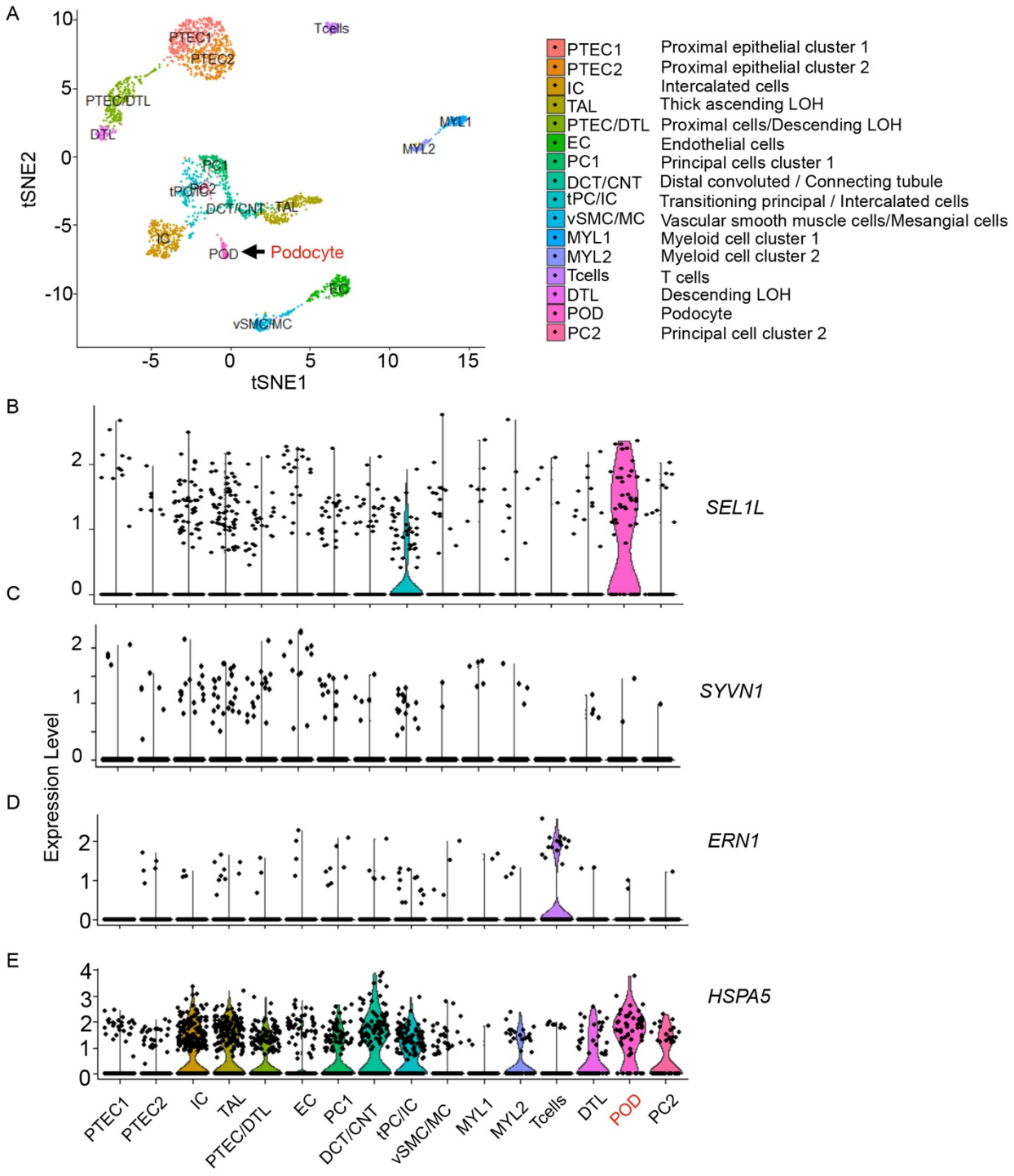

**Figure S2. SEL1-HRD1 ERAD expression in FSGS human kidneys.** Representative confocal images of SEL1L (**A**) and HRD1 (**B**) staining in kidneys from healthy and FSGS humans, co-stained with WT1. Asterisks, WT1 positive podocytes. Healthy 1 and 2 were used as the controls for FSGS1 and FSGS 2/3, respectively, with quantitation of SEL1L and HRD1 shown in **(C-D)**. (**C**), Healthy1, n=103 podocytes from 5 glomeruli; FSGS1, n=62 from 5 glomeruli; Healthy2, n=134 from 5 glomeruli; FSGS2, n=53 from 4 glomeruli; FSGS3, n=48 from 3 glomeruli. **(D)**, Healthy1, n=121 from 5 glomeruli; FSGS1, n=81 from 5 glomeruli; Healthy2, n=137 from 5 glomeruli; FSGS2, n=47 from 4 glomeruli; FSGS3, n=72 from 4 glomeruli. Values are shown as the mean ± SEM. n.s., not significant; ***, *P*<0.001 by the Kruskal-Wallis H test.

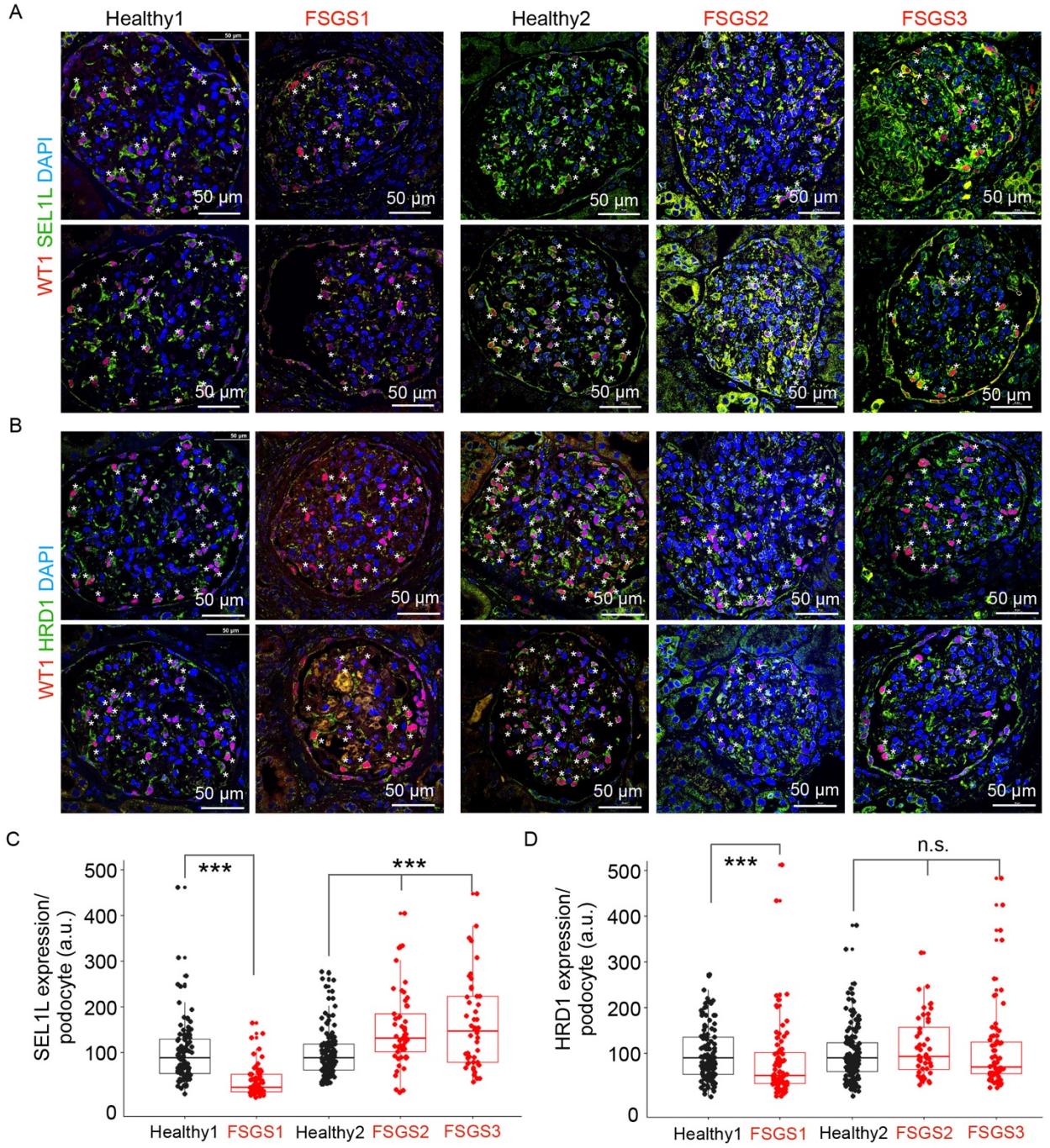

**Figure S3. Early onset of proteinuria in *Sel1L*$^{PodCre}$ mice. (A, B, E)** SDS-PAGE analysis followed by Coomassie brilliant blue staining of urine (0.5 µl per lane) obtained from Sel1L cohorts (**A**) or IRE1α cohorts (**E**) at indicated ages. 0.5 and 5 µg BSA, loading controls. Quantitation is shown in **(B)**. **(C)** Serum concentration of BUN in 3-, 5-, 7-, 10-week-old *Sel1L*$^{f/f}$ and *Sel1L*$^{PodCre}$ mice (n=9, 11 at 3 w; 11, 9 at 5 w; 6, 8 at 7 w; 5, 4 at 10 w). **(D)** Serum concentration of ALT in 3-, 5-, 7-, 10-week-old *Sel1L*$^{f/f}$ and *Sel1L*$^{PodCre}$ mice (n=9, 8 at 3 w; 9, 7 at 5 w; 6, 8 at 7 w; 6, 6 at 10 w). **(F-G)** Quantitation of glomeruli size (**F**) and mesangial index (**G**) from 5-week-old *Sel1L*$^{f/f}$ and *Sel1L*$^{PodCre}$ mice (60 glomeruli from 3 mice each). Each symbol represents each glomerulus. Values are shown as the mean ± SEM. n.s., not significant, *, $P$<0.05, **, $P$<0.001, ***, $P$<0.0001 by two-tailed Student's t test and one-way ANOVA were used for 3-7 and 10 w, respectively.

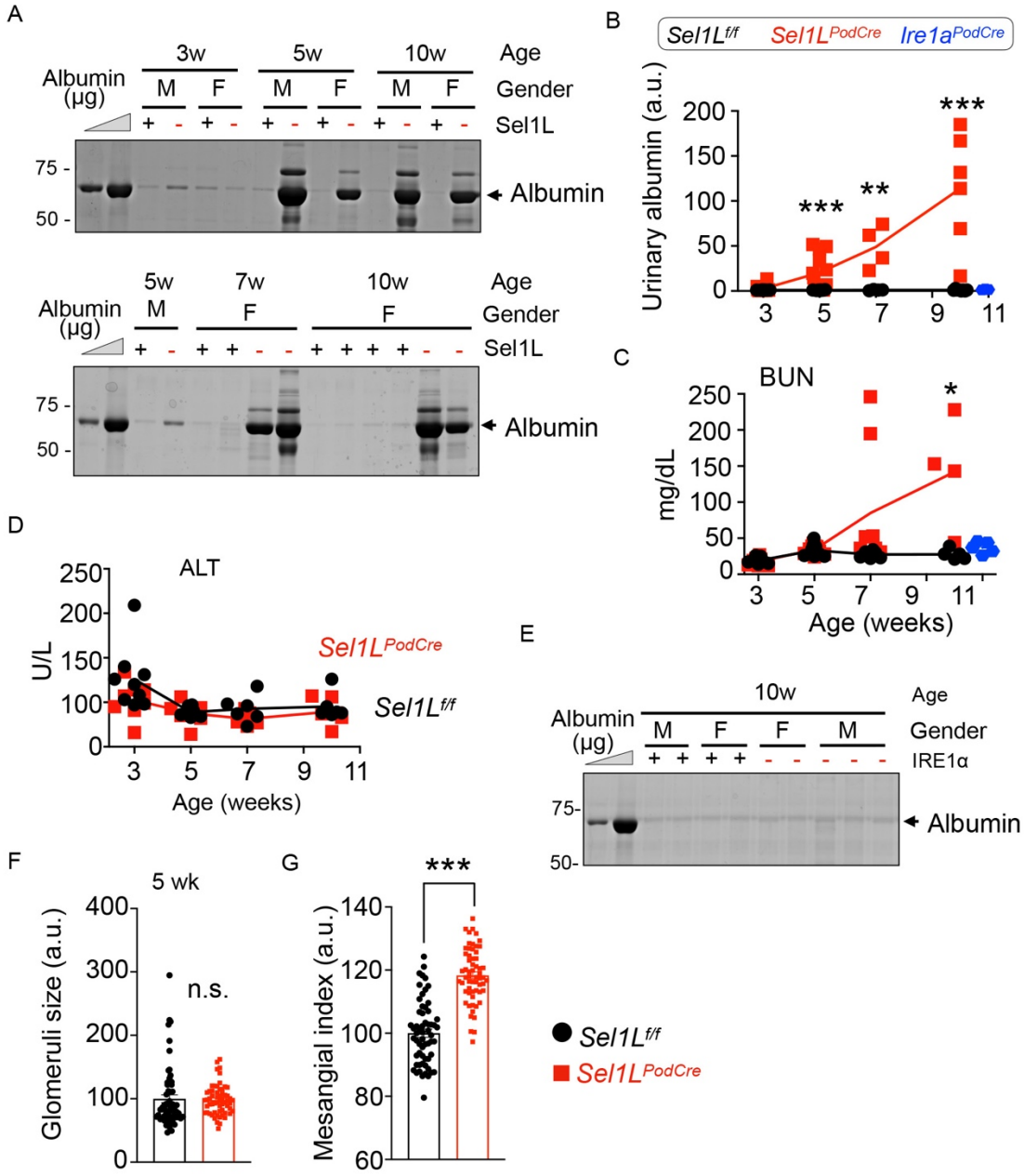

**Figure S4. Sel1L is required for the formation of foot process and slit diaphragm.** Additional image sets of SEM (**A-C**) and TEM (**D-E**) of Fig. 4A-E from another set of mice. CB, cell body of podocytes; PP, primary process; SP, secondary process; FP, foot process; GBM, glomerular basement membrane; Endo, endothelial cells; ER, endoplasmic reticulum; CL, capillary lumen; US, urinary space. (**F**) Quantitation of the length of slit diaphragm in wildtype mice of **Fig. 4F** (n=153 slit diaphragms from 6 glomeruli of two 5-week-old mice).

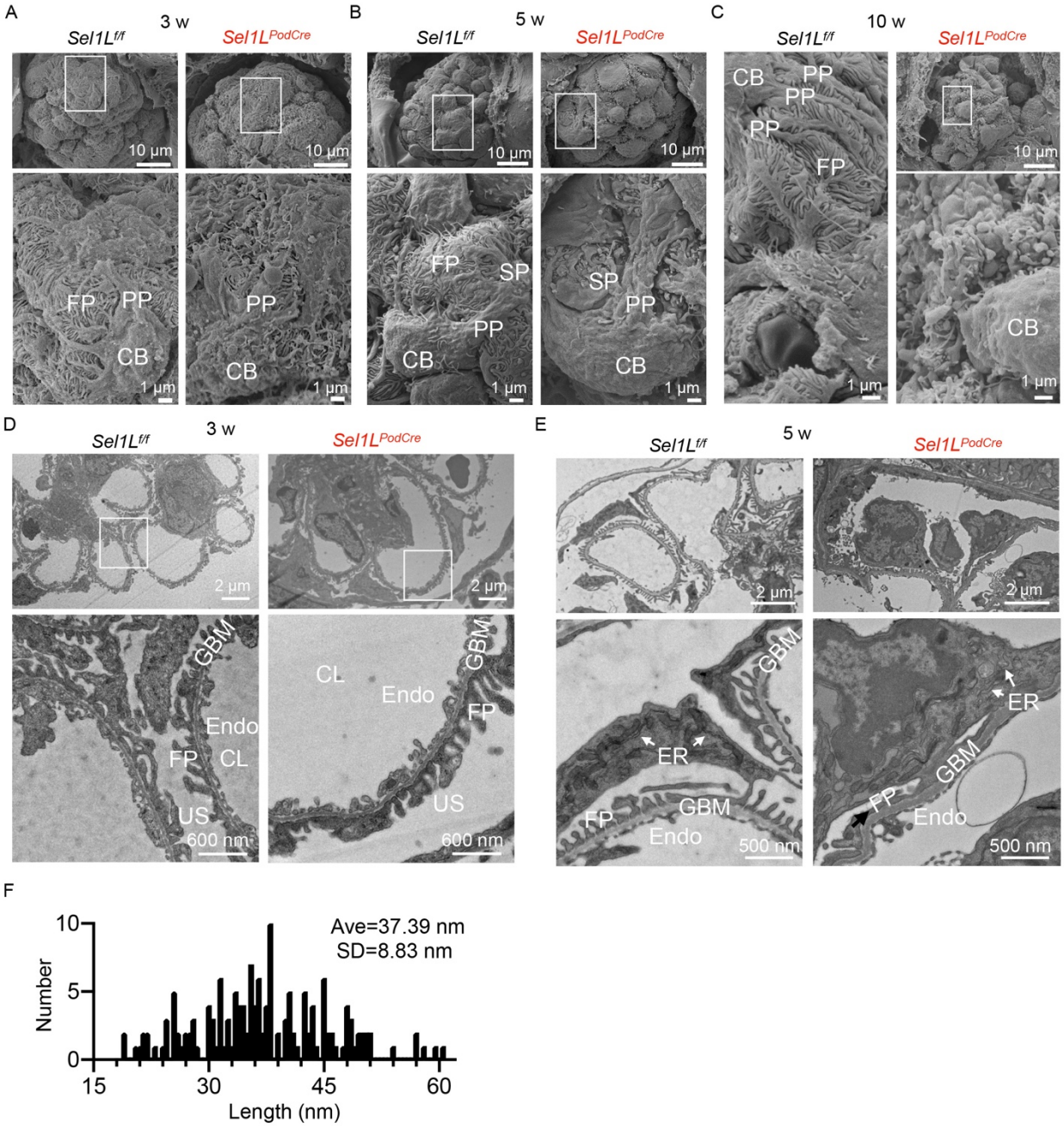

**Figure S5. Sel1L is required for the formation of slit diaphragm.** (**A**) Images of the same podocyte from a 5-week-old *Sel1L*$^{PodCre}$ mouse taken from regular vs. ultra-high-resolution SEM. (**B-C**) Additional ultra-high-resolution SEM images from another set of 5-week-old mice.

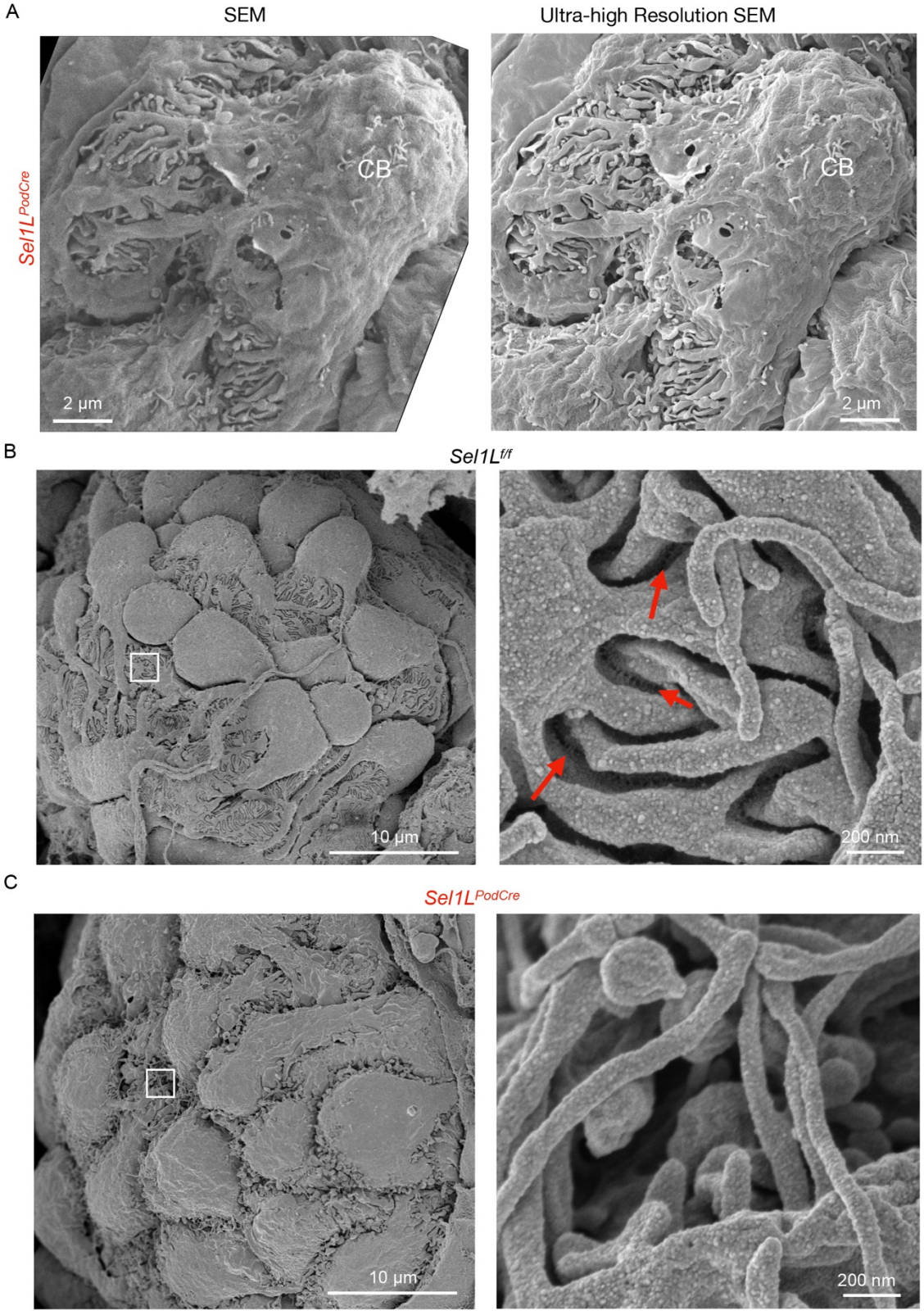

**Figure S6. Sel1L deficiency alters nephrin maturation. (A)** The same image as **Fig. 5A** with enhanced KDEL signals to show the co-localization of nephrin in the ER of *Sel1L*$^{f/f}$ podocytes (arrows). (**B**) Representative confocal images of synaptopodin-BiP in kidney sections of 3-week-old mice (*n*=3). **(C)** Western blot of nephrin levels in purified microsomal fractions of 3-week-old *Sel1L*$^{f/f}$ and *Sel1L* $^{PodCre}$ mice, with quantitation shown below the gel. (n=3). **(D)** Quantitation of percent of nephrin resistant (r) and sensitive (s) in total nephrin shown in **Fig. 5H** (n=5 mice each group). (**E**) Western blot analysis of podocin and synaptopodin in kidney lysates from 3, 5 and 7-week-old *Sel1L*$^{f/f}$ and *Sel1L* $^{PodCre}$ mice, with quantitation shown below the gel. Values are shown as the mean ± SEM. **P*<0.05, by two-tailed Student's t test.

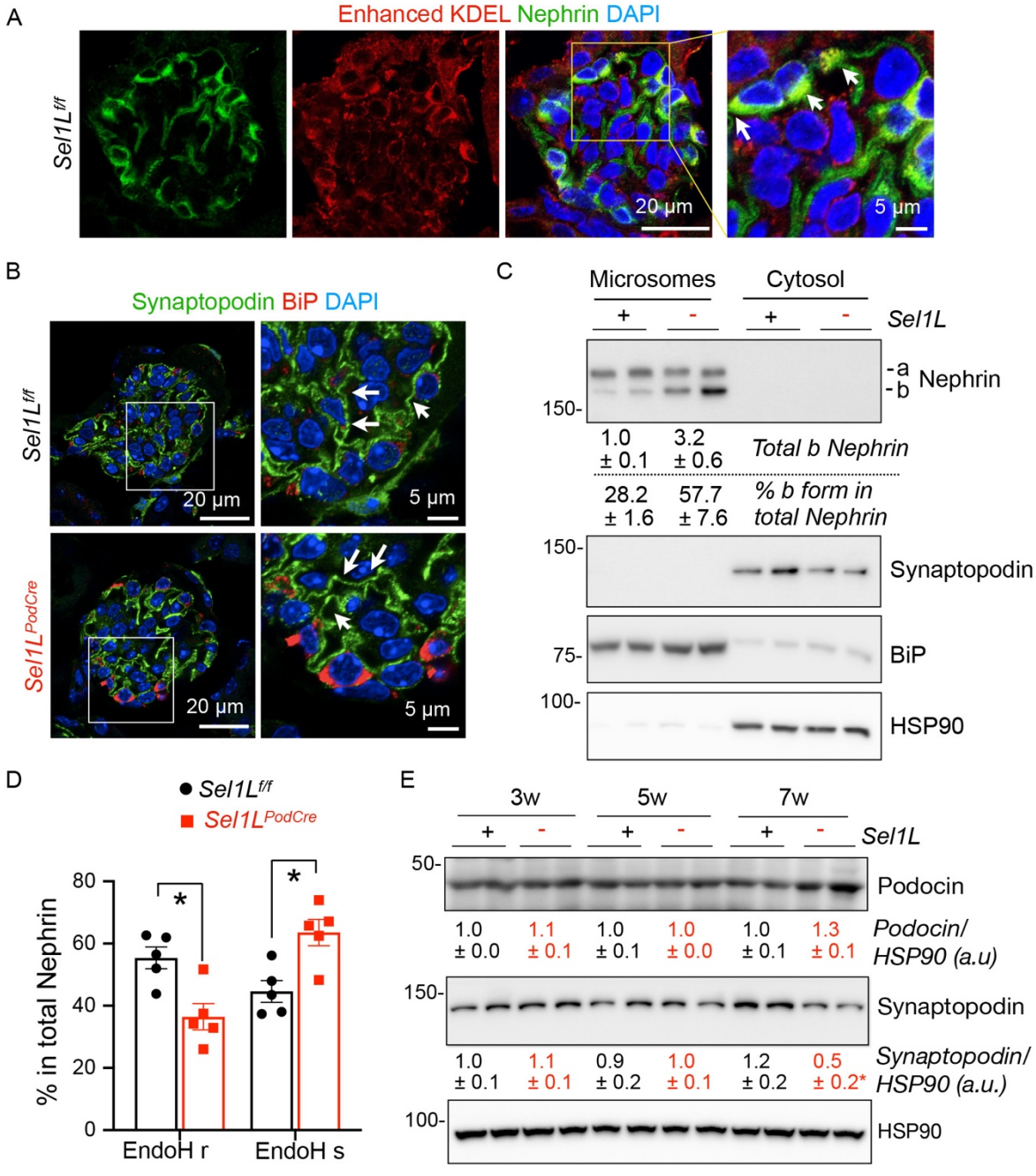

**Figure S7. *Ire1a* deficiency has no effect on nephrin distribution and maturation in podocytes.** (**A-B**) Western blot analysis in kidney lysates from 3, 5 and 7-week-old mice (*Ire1a*$^{f/f}$ vs *Ire1a*$^{PodCre}$), with *Sel1L*$^{PodCre}$ mice as controls in A. (**C**) Representative confocal images of nephrin-KDEL in kidney sections of 3-week-old mice (*Ire1a*$^{f/f}$ vs *Ire1a*$^{PodCre}$) (*n*=3). Arrows, mature nephrin along the GBM.

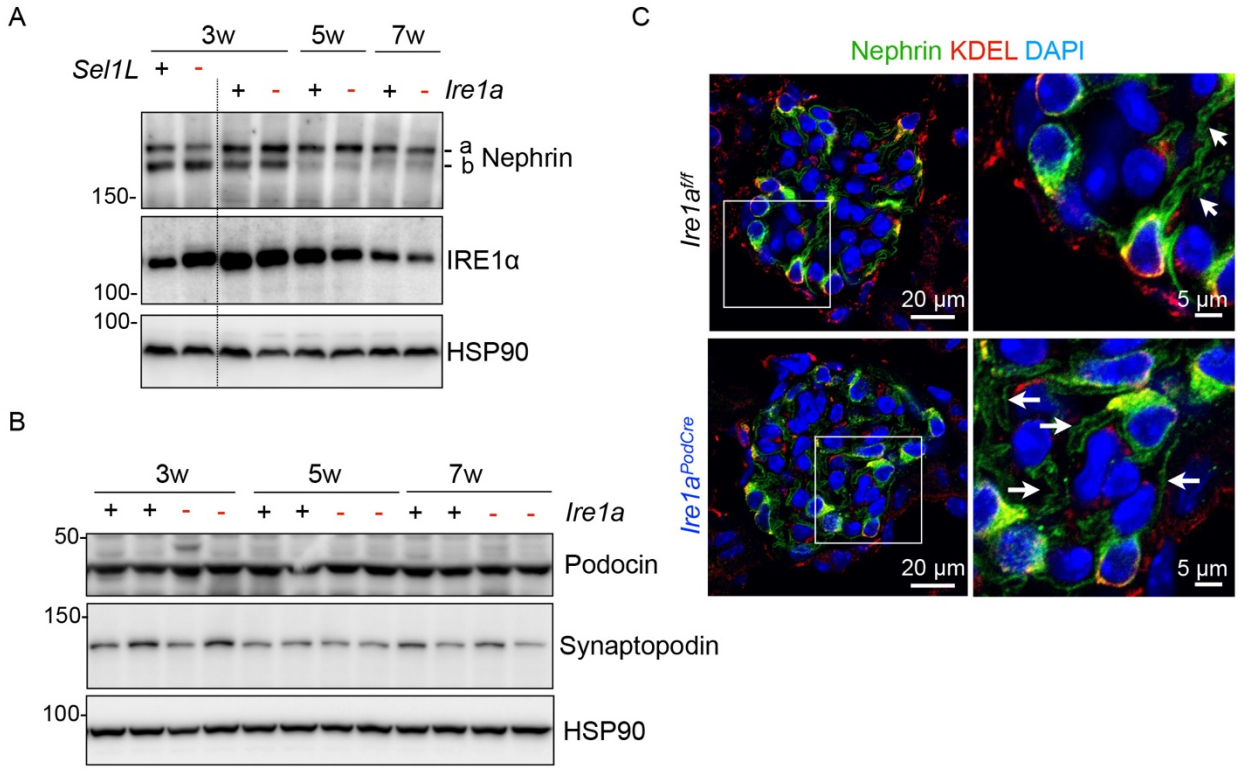

**Figure S8. Sel1L-Hrd1 ERAD controls nephrin maturation.** (**A**) Western blot analysis of nephrin in transfected HEK293T cells in a six-well plate, showing that HRD1 overexpression rescued the maturation defects of nephrin in *HRD1*-deficient cells. Quantitation from three independent experiments shown below. Values are shown as the mean ± SEM. ***, *P*<0.0001 by two-tailed Student's t test. (**B**) Western blot analysis of ubiquitination following immunoprecipitation of nephrin or GFP (control) in HEK293T cells transfected with nephrin or GFP, together with wildtype or mutant C2A HRD1. Data are representative of at least 2 independent experiments.

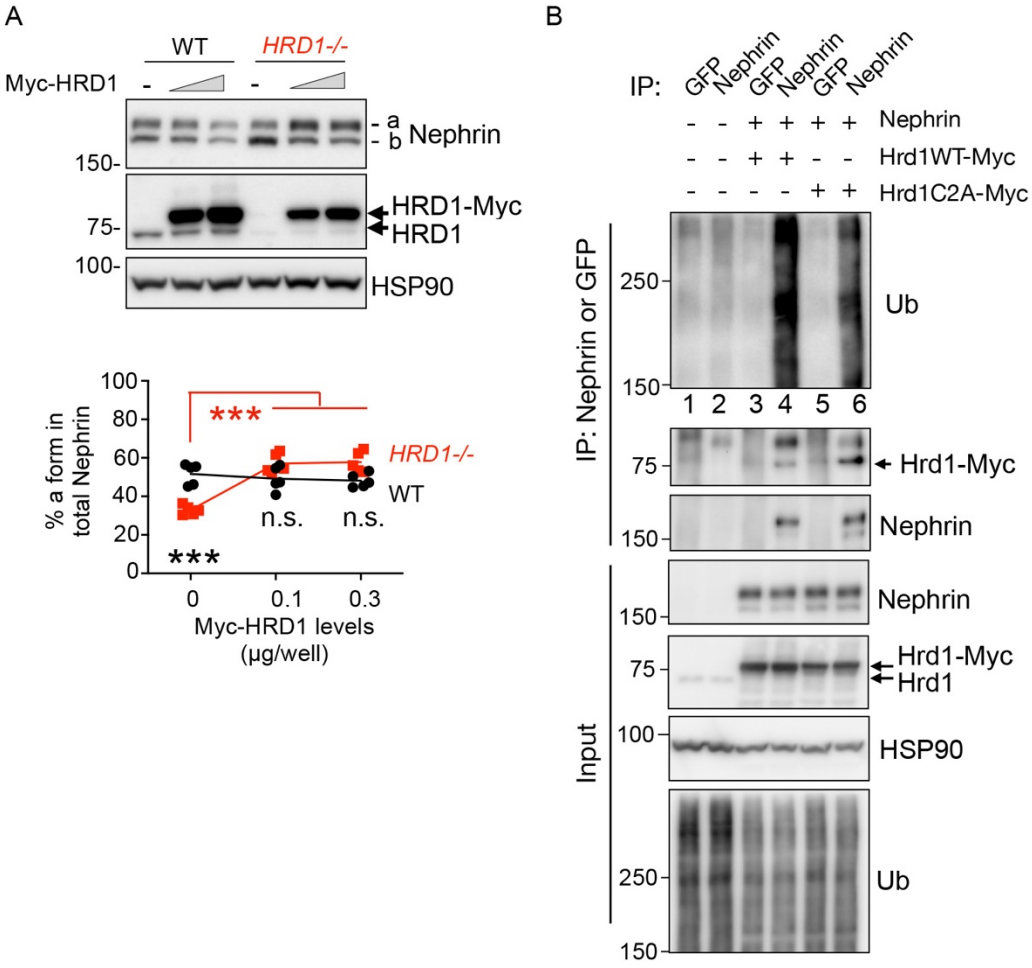

**Figure S9. Predicated local structures and ER retention of nephrin mutants. (A-D)** Predicted local structures of WT (upper) and nephrin mutants (lower). WT and mutated amino acids were labeled in green and magenta, respectively. S366R introduces excessive positive charges in the local region (A). S724C may result in additional disulfide bond with other proteins (B). R743C disrupts original disulfide bond between C816 and C761 (C). L832P may change the backbone orientation of the beta-sheet indicated by the arrow (D). (**E**) Western blot analysis of nephrin following EndoH digestion in HEK293T cells transfected with WT or mutant nephrin. (**F**) Representative confocal images of nephrin-KDEL staining in HEK293T cells expressing G270C nephrin, showing the ER retention of the mutant (arrows).

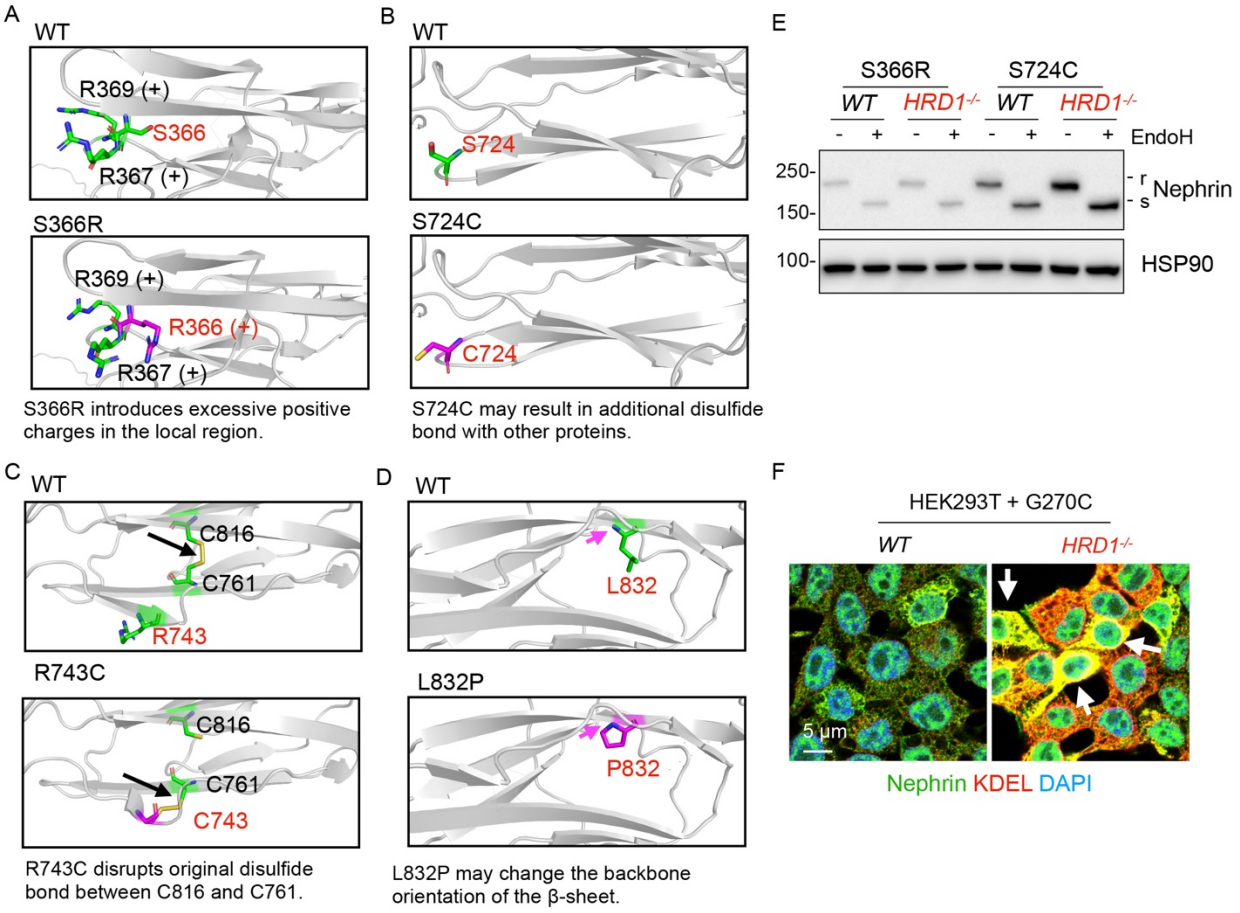

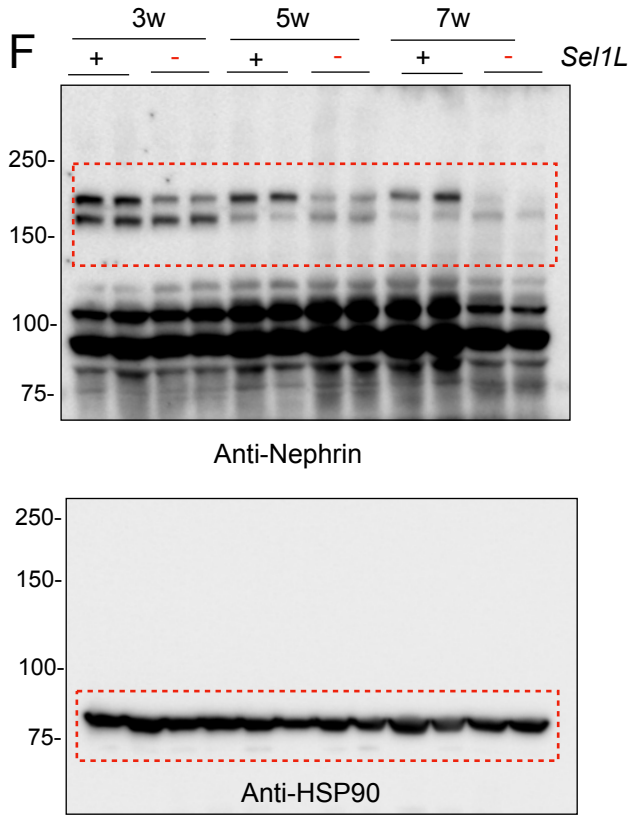


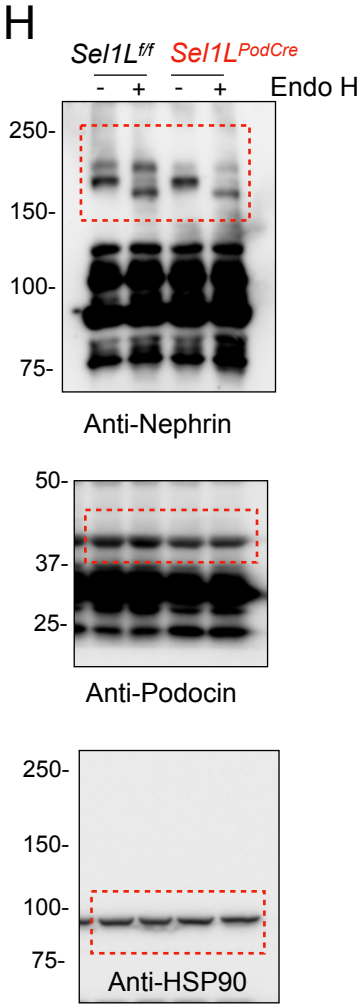


Full unedited gel for Figure 5

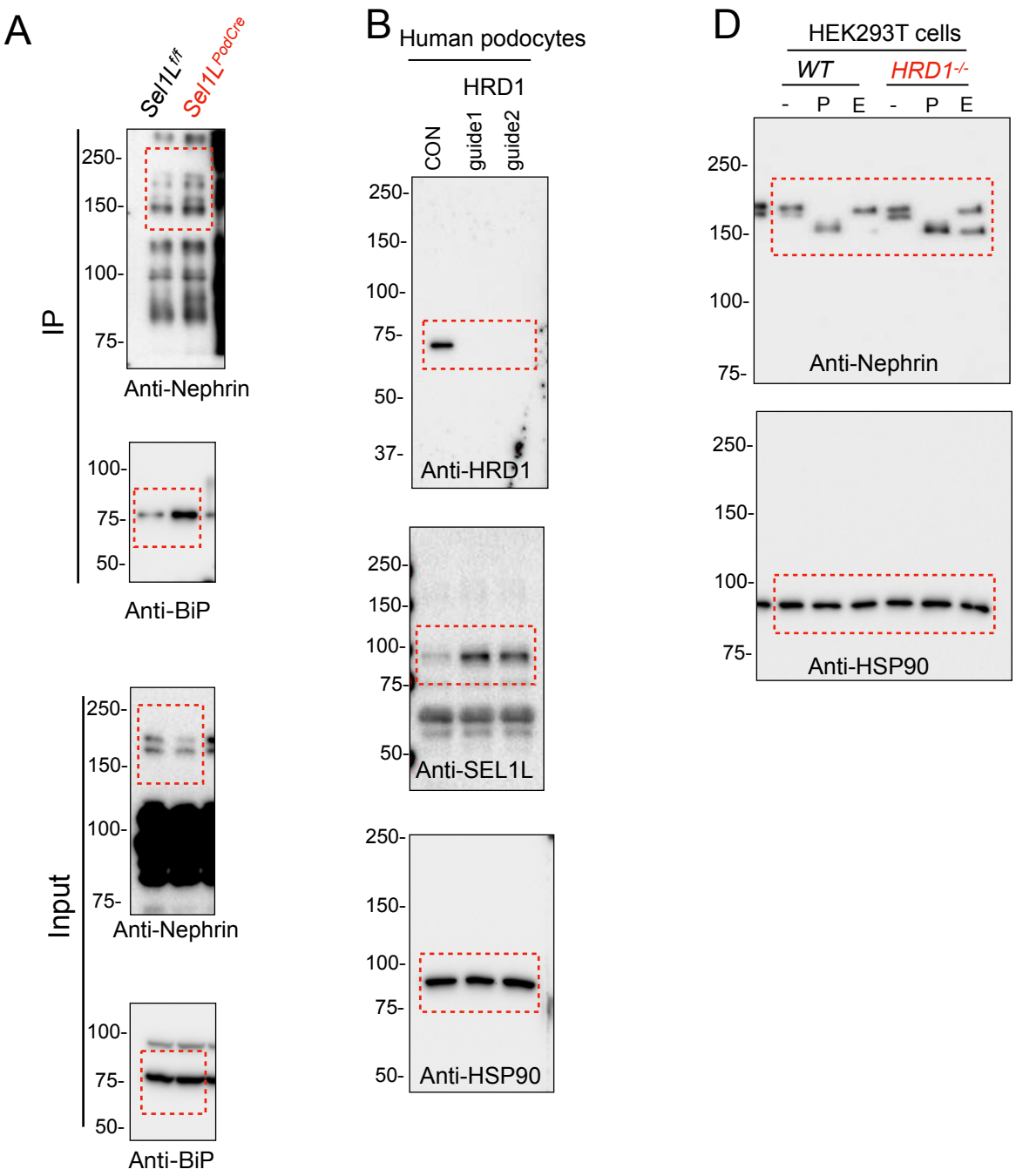


Full unedited gel for Figure 6A-D

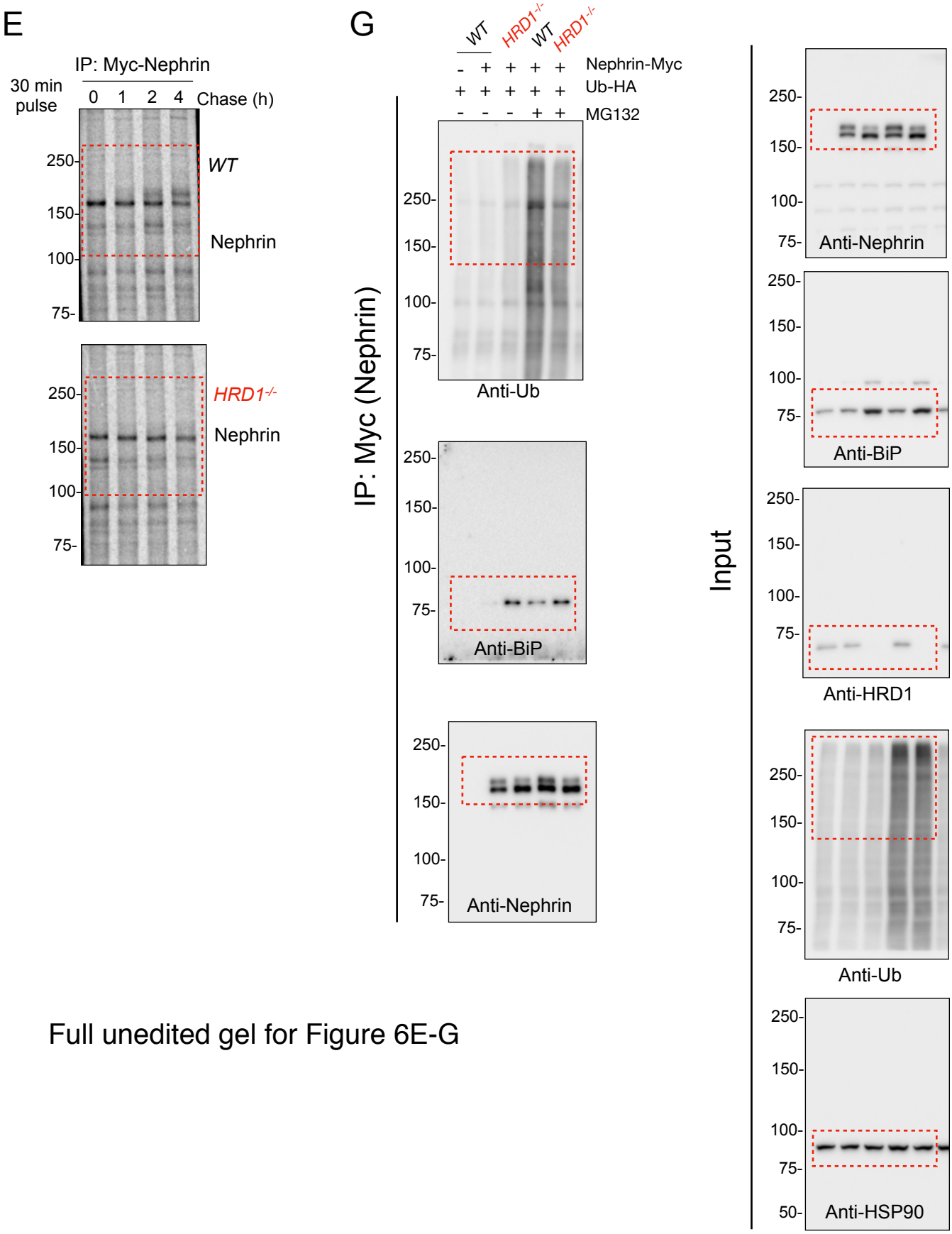


Full unedited gel for Figure 6E-G

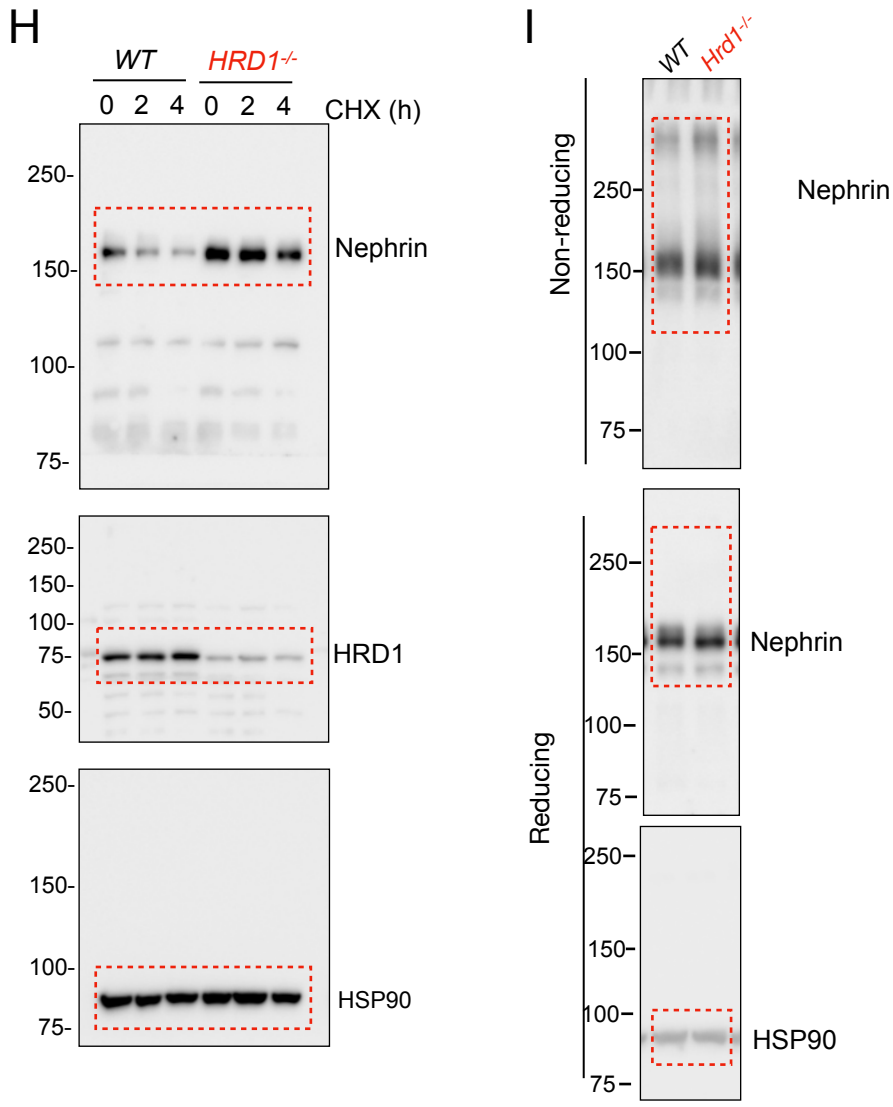


Full unedited gel for Figure 6H-I

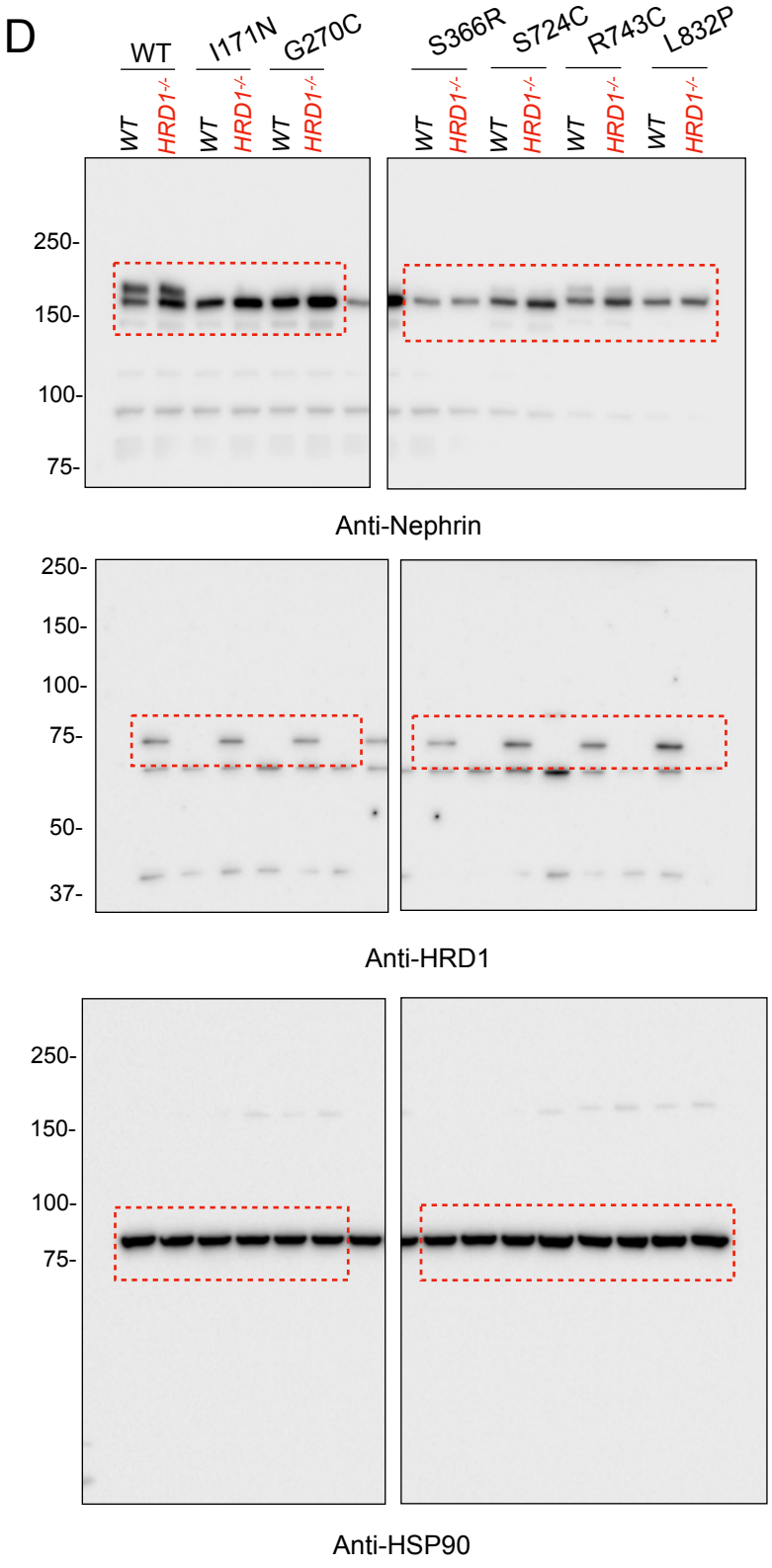


Full unedited gel for Figure 7D

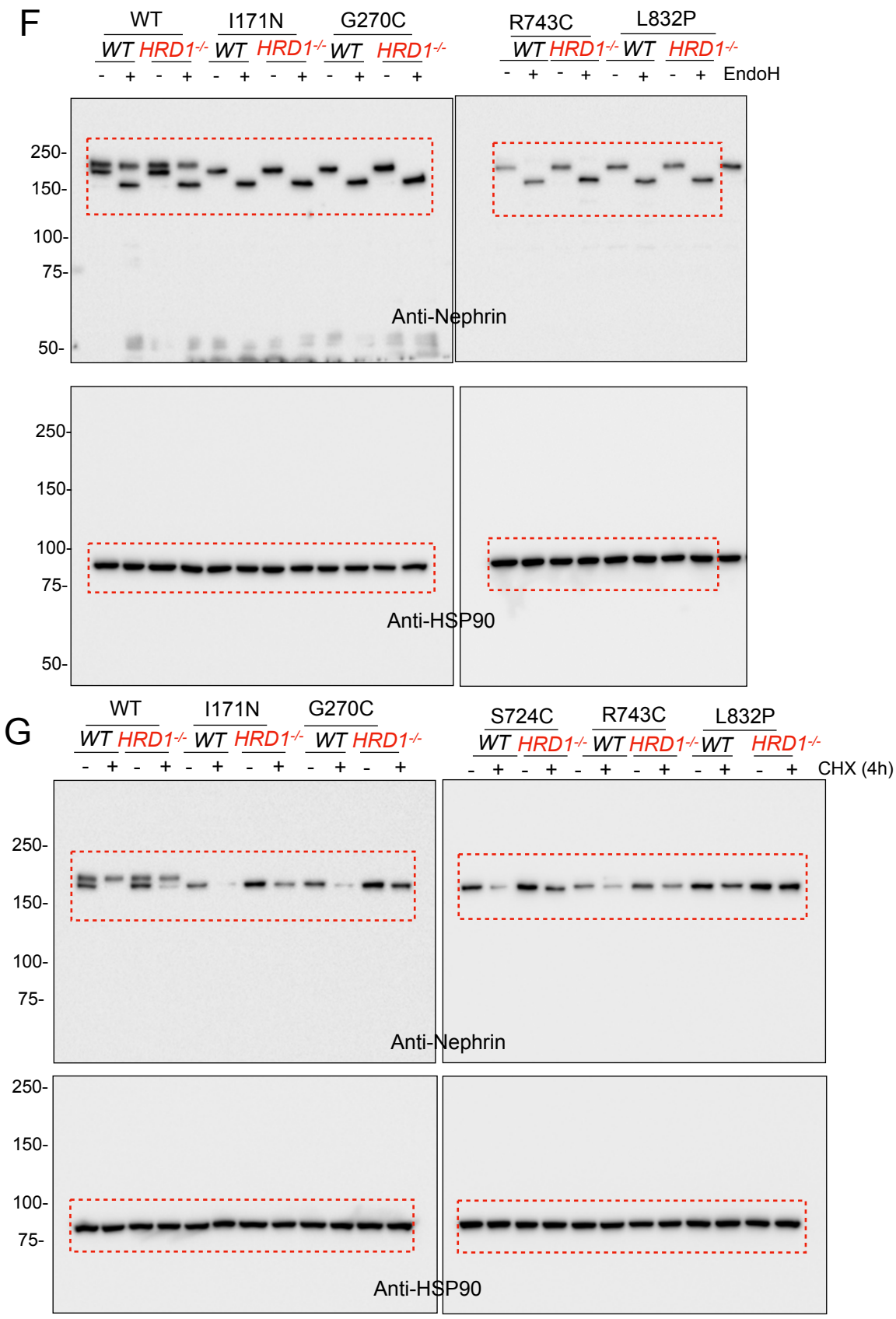


Full unedited gel for Figure 7F-G

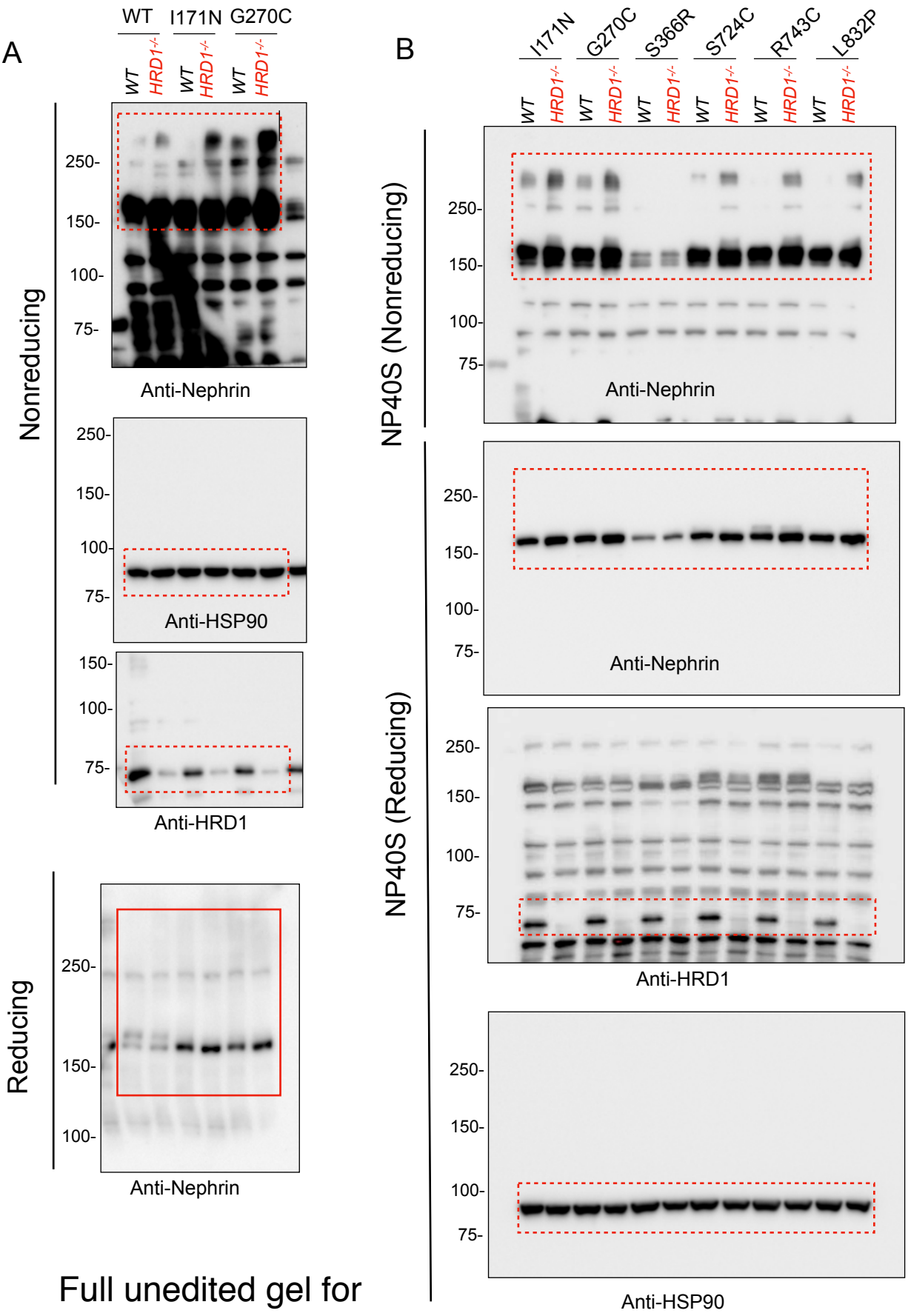


Full unedited gel for Figure 8A-B

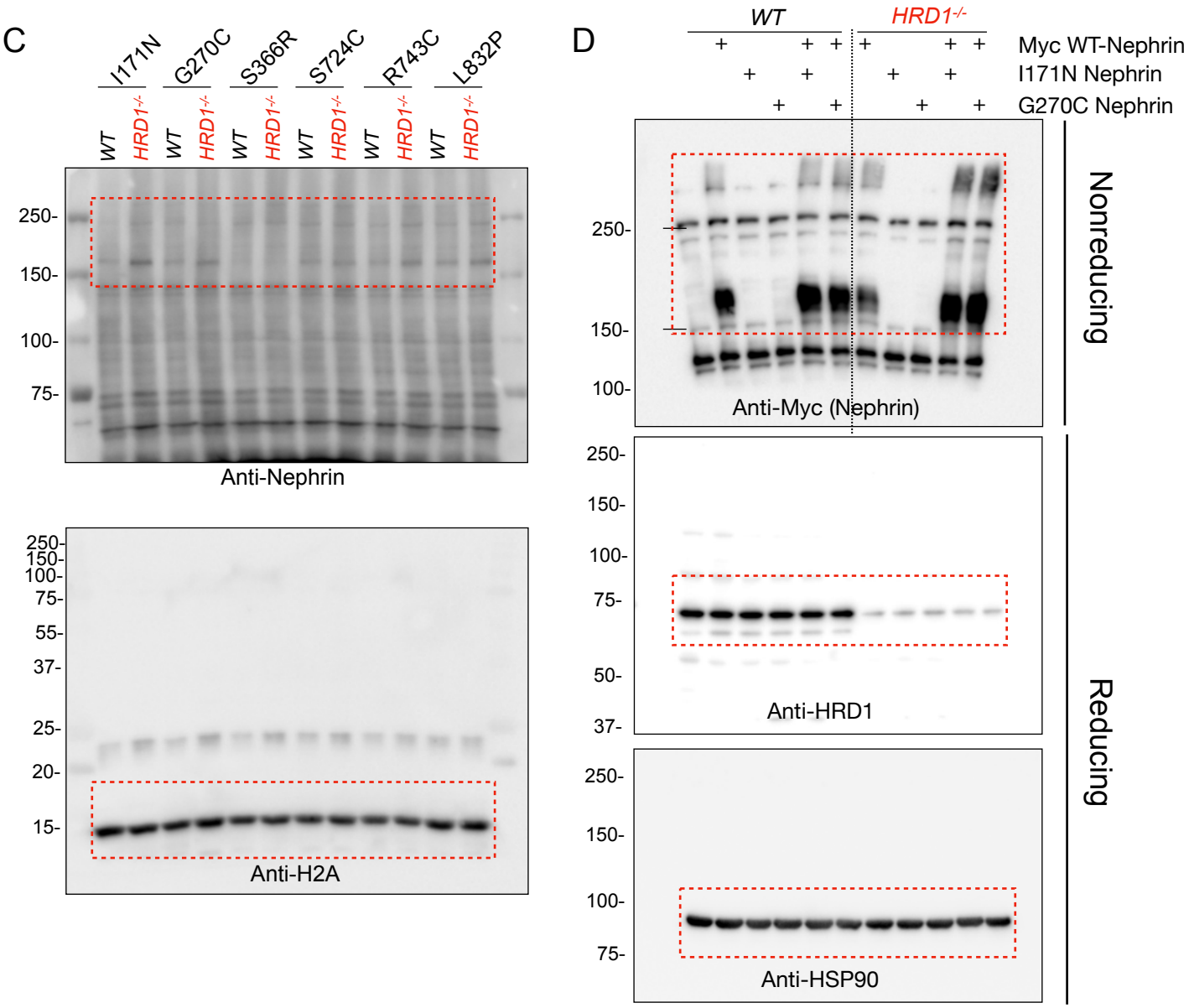


Full unedited gel for Figure 8C-D

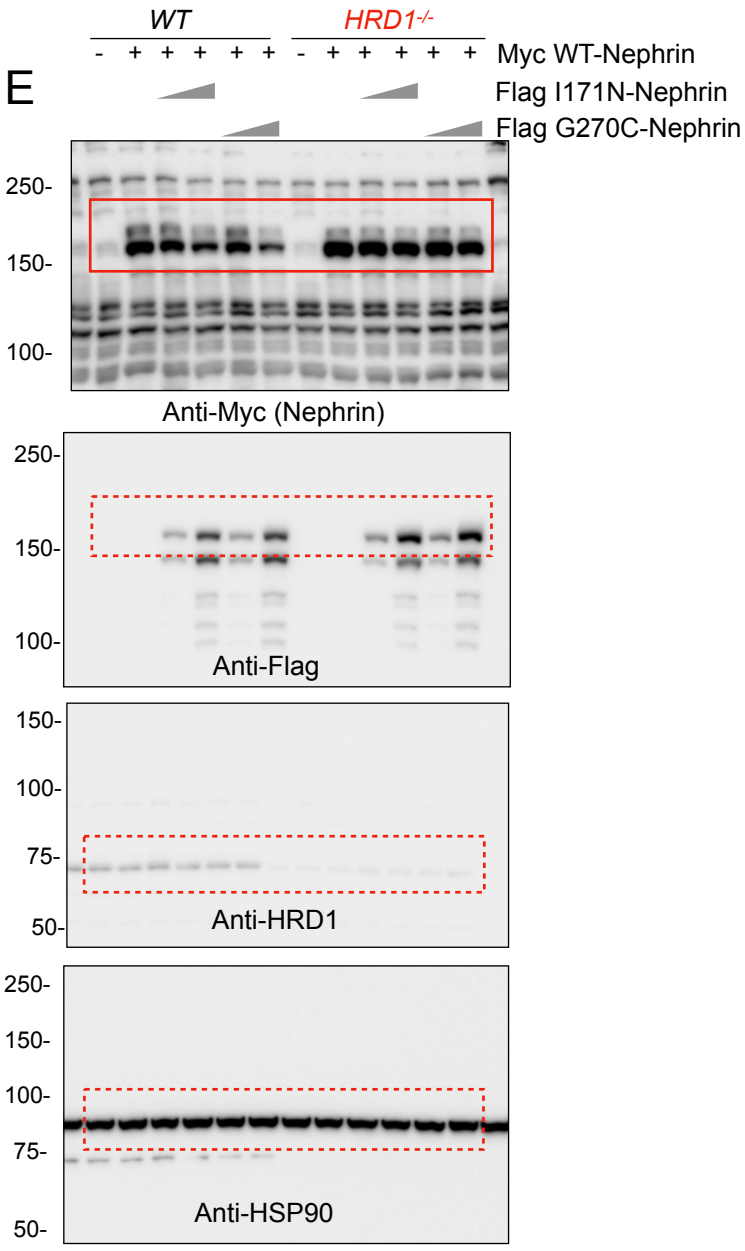


Full unedited gel for Figure 8E

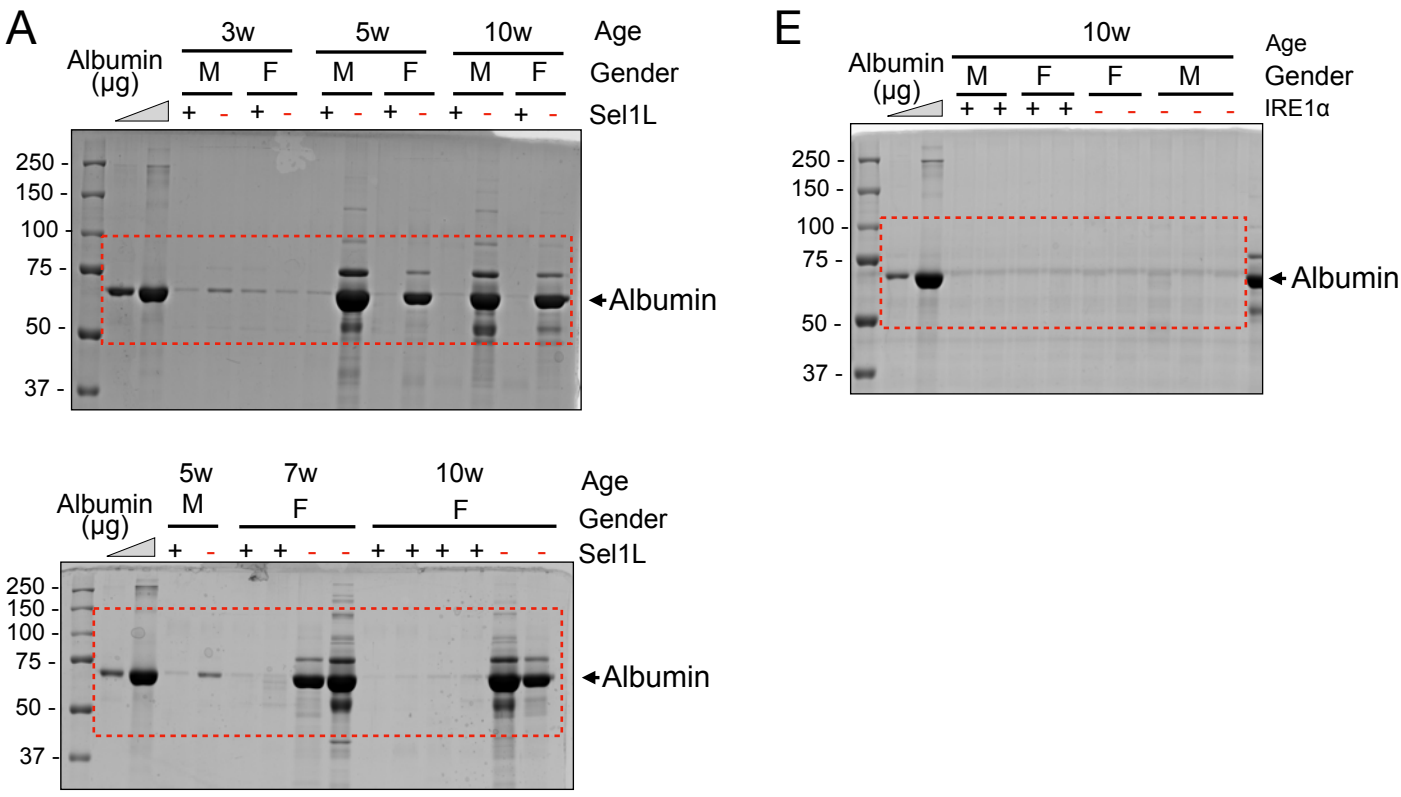


Full unedited gel for Figure S3

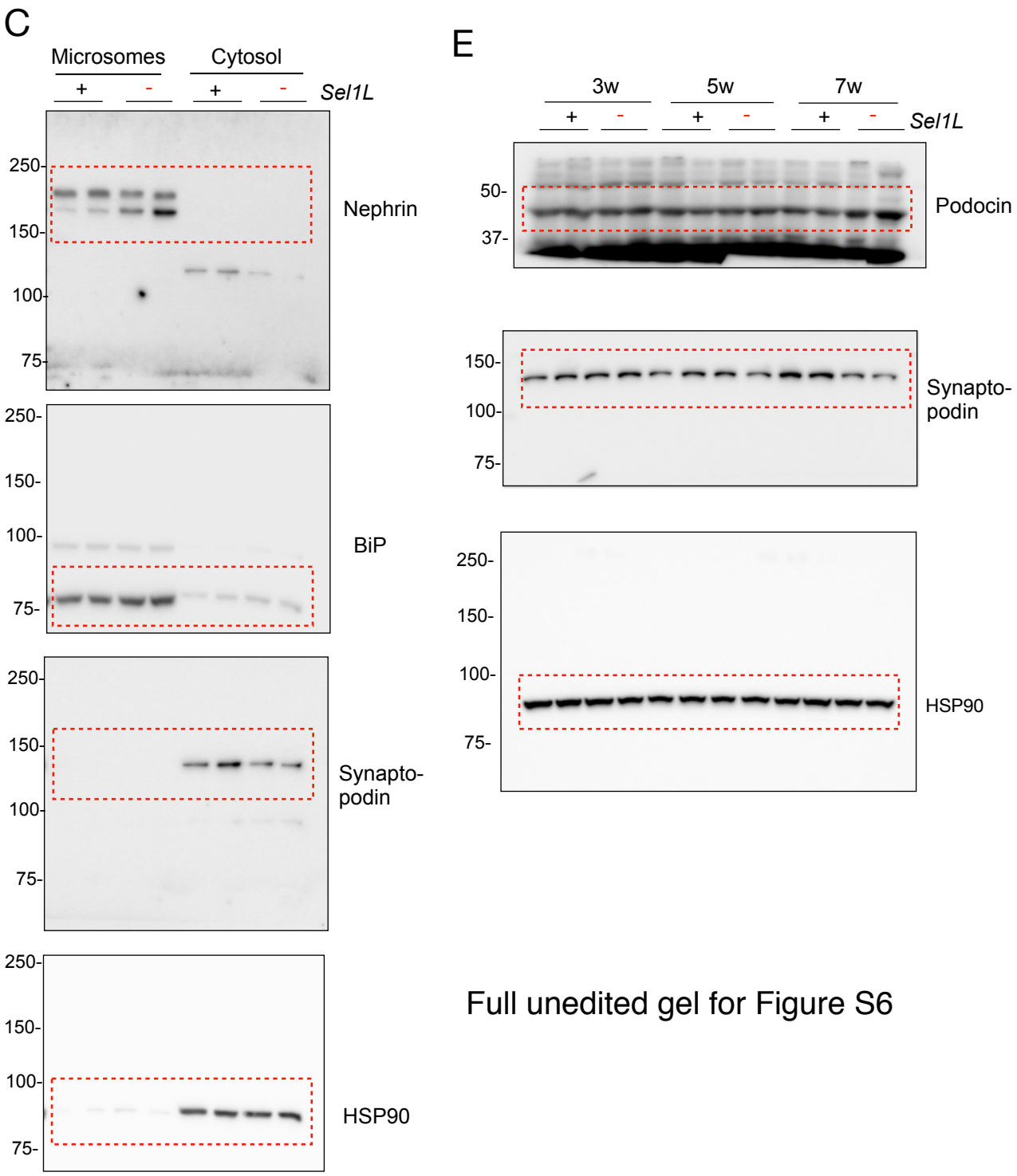


Full unedited gel for Figure S6

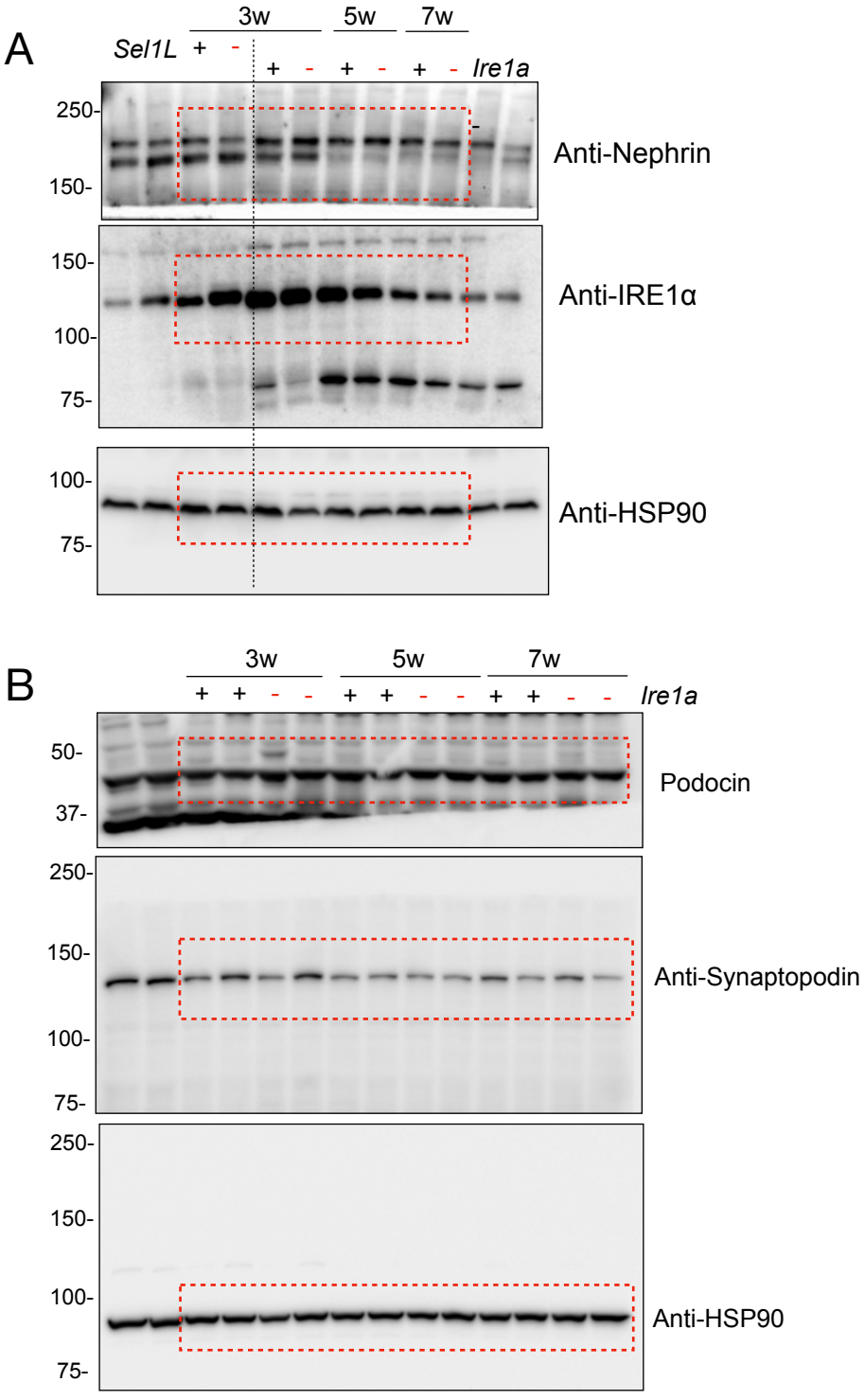


Full unedited gel for Figure S7

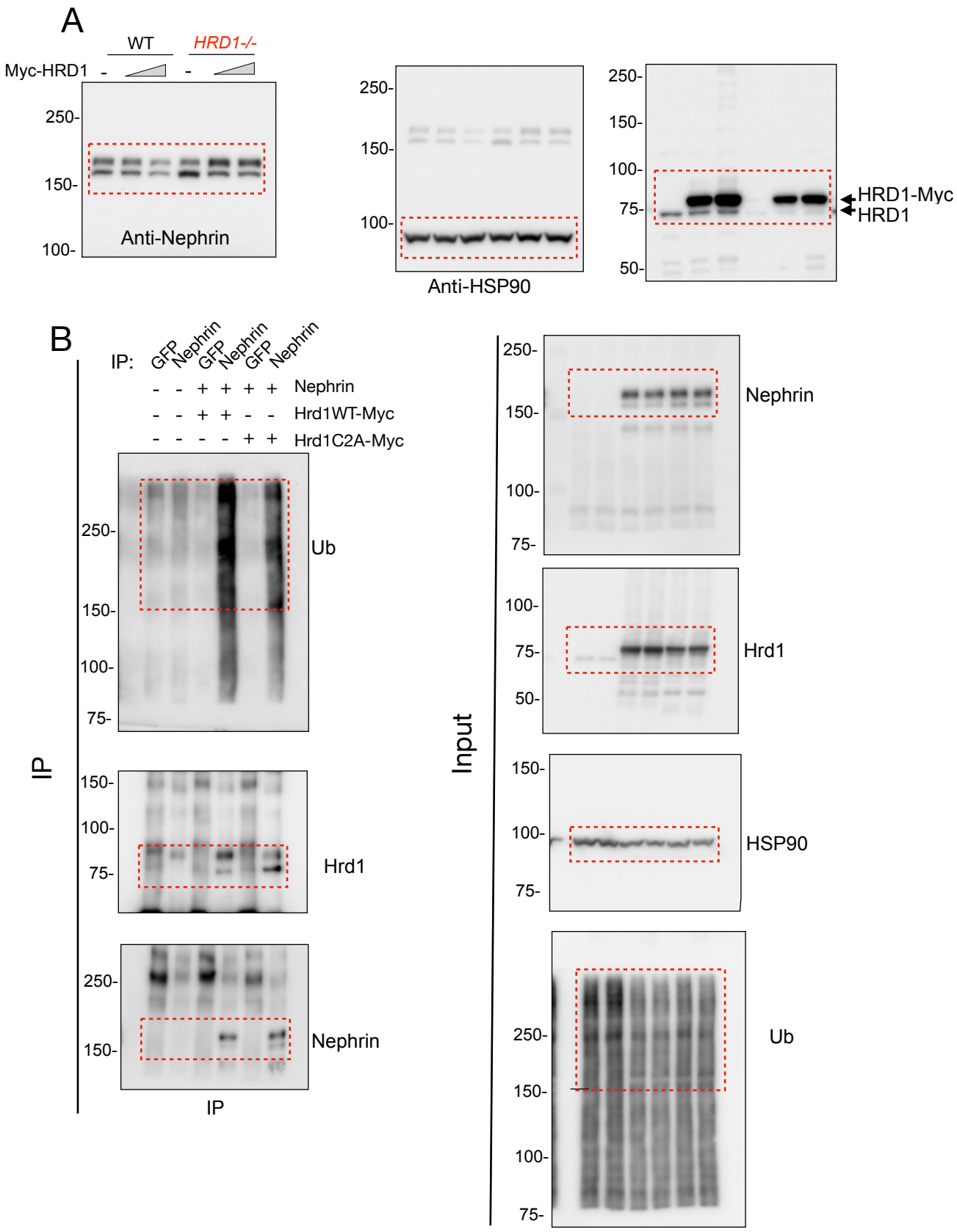


Full unedited gel for Figure S8

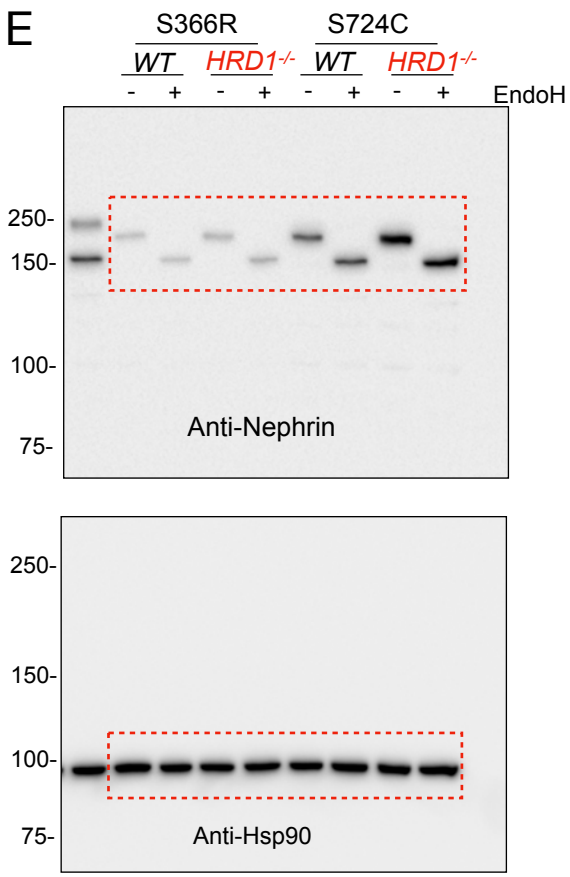


Full unedited gel for Figure S9